

Experimental violation of a Bell-like inequality with optical vortex beams

This content has been downloaded from IOPscience. Please scroll down to see the full text.

2015 New J. Phys. 17 113046

(<http://iopscience.iop.org/1367-2630/17/11/113046>)

View [the table of contents for this issue](#), or go to the [journal homepage](#) for more

Download details:

IP Address: 147.96.14.16

This content was downloaded on 22/01/2016 at 19:32

Please note that [terms and conditions apply](#).



PAPER

OPEN ACCESS

RECEIVED

29 May 2015

REVISED

22 October 2015

ACCEPTED FOR PUBLICATION

27 October 2015

PUBLISHED

17 November 2015

Content from this work
may be used under the
terms of the [Creative
Commons Attribution 3.0
licence](#).

Any further distribution of
this work must maintain
attribution to the
author(s) and the title of
the work, journal citation
and DOI.



Experimental violation of a Bell-like inequality with optical vortex beams

B Stoklasa¹, L Motka¹, J Rehacek¹, Z Hradil¹, L L Sánchez-Soto^{2,3} and G S Agarwal⁴¹ Department of Optics, Palacký University, 17. listopadu 12, 771 46 Olomouc, Czech Republic² Departamento de Óptica, Facultad de Física, Universidad Complutense, 28040 Madrid, Spain³ Max-Planck-Institut für die Physik des Lichts, Günther-Scharowsky-Straße 1, Bau 24, 91058 Erlangen, Germany⁴ Department of Physics, Oklahoma State University, Stillwater, Oklahoma 74078, USA**Keywords:** classical entanglement, optical beams, Bell tests, non-separability

Abstract

Optical beams with topological singularities have a Schmidt decomposition. Hence, they display features typically associated with bipartite quantum systems; in particular, these classical beams can exhibit entanglement. This classical entanglement can be quantified by a Bell inequality formulated in terms of Wigner functions. We experimentally demonstrate the violation of this inequality for Laguerre–Gauss (LG) beams and confirm that the violation increases with increasing orbital angular momentum. Our experimental scheme, which is designed to give directly the parity of the Wigner function, yields negativity at the origin for LG₁₀ beams, whereas for LG₂₀ we always get a positive value.

1. Introduction

Entanglement is usually presented as one of the weirdest features of quantum theory that departs strongly from our common sense [1]. Since the seminal work of Einstein, Podolsky and Rosen (EPR) [2], countless discussions on this subject have popped up [3].

A major step in the right direction was due to Bell [4], who formulated the EPR dilemma in terms of an inequality which naturally led to a falsifiable prediction. Actually, it is common to use an alternative formulation, derived by Clauser, Horne, Shimony and Holt (CHSH) [5], which is better suited for realistic experiments.

The main stream of research [6, 7] settled the main concepts of this topic in the realm of quantum physics. However, in recent years a general consensus has been reached on the fact that entanglement is not necessarily a signature of the quantumness of a system. Actually, as aptly remarked in [8], one should distinguish between two types of entanglement: between spatially separated systems (inter-system entanglement) and between different degrees of freedom of a single system (intra-system entanglement). Inter-system entanglement occurs only in truly quantum systems and may yield nonlocal statistical correlations. Conversely, intra-system entanglement may also appear in classical systems and cannot generate nonlocal correlations [9, 10]; for this reason, it is often dubbed as ‘classical entanglement’. Since its introduction by Spreeuw [11], this notion has been employed in a variety of contexts [12].

Classical entanglement has allowed testing of Bell inequalities with classical wave fields. The physical significance of this violation is not linked to quantum nonlocality, but rather points to the impossibility of constructing such a beam using other beams with uncoupled degrees of freedom. However, all the experiments conducted thus far to observe this violation have involved only discrete variables, such as spin and beam paths of single neutrons [13], polarization and transverse modes of a laser beam [14–20], different transverse modes propagating in multimode waveguides [21], polarization of two classical fields with different frequencies [22], orbital angular momentum [23, 24], and polarization and spatial parity [25].

In this paper, we continue the analysis of this classical entanglement by focusing on the simple but engaging example of vortex beams. To this end, in section 2 we revisit a decomposition of Laguerre–Gauss (LG) beams in the Hermite–Gauss (HG) basis that can be rightly interpreted as a Schmidt decomposition. This immediately

suggests that many ideas ensuing from the quantum world may be applicable to these beams as well. In particular, in section 3 we address the inseparability of the LG modes using a CHSH violation that we quantify in terms of the associated Wigner function. As this distribution can be understood as a measure of the displaced parity, in section 4 we discuss an experimental realization which nicely agrees with the theoretical predictions. Finally, our conclusions are summarized in section 5.

2. Optical vortices and Schmidt decomposition

It is well known that the beam propagation along the z direction of a monochromatic scalar field of frequency ω ; i.e., $E(\mathbf{r}, t) = \mathcal{E}(\mathbf{r})\exp[-i(\omega t - kz)]$, is governed by the paraxial wave equation

$$i\frac{\partial \mathcal{E}}{\partial z} = -\frac{\lambda}{2}\left(\frac{\partial^2}{\partial x^2} + \frac{\partial^2}{\partial y^2}\right)\mathcal{E}, \quad (2.1)$$

with $\lambda = \lambda/2\pi$ where λ is the wavelength. Equation (2.1) is formally identical to the Schrödinger equation for a free particle in two dimensions, with the obvious identifications $t \mapsto z$, $\psi \mapsto \mathcal{E}$, and $\hbar \mapsto \lambda$.

Any optical beam can be thus expressed as a superposition of fundamental solutions of equation (2.1). In Cartesian coordinates, a natural orthonormal set is given by the Hermite–Gauss (HG) modes:

$$\text{HG}_{mn}(x, y) = \sqrt{\frac{2}{\pi n! m! 2^{n+m}}} \left(\frac{1}{w}\right) H_m\left(\frac{\sqrt{2}x}{w}\right) H_n\left(\frac{\sqrt{2}y}{w}\right) \exp\left(-\frac{x^2 + y^2}{w^2}\right), \quad (2.2)$$

where w is the beam waist, and H_m are the Hermite polynomials. Note that we are restricting ourselves to the plane $z = 0$, since we are not interested here in the evolution. We will use the set (2.2) for the Schmidt decomposition of Laguerre–Gauss beams.

For cylindrical symmetry, it is convenient to use the set of Laguerre–Gauss (LG) modes, which contain optical vortices with topological singularities; they read

$$\text{LG}_{mn}(r, \varphi) = \sqrt{\frac{2}{\pi m! n!}} \min(m, n)! (-1)^{\min(m, n)} \left(\frac{1}{w}\right) \times \left(\frac{\sqrt{2}r}{w}\right)^{|m-n|} L_{\min(m, n)}^{|m-n|}\left(\frac{2r^2}{w^2}\right) \exp\left(-\frac{r^2}{w^2}\right) \exp[i(m-n)\varphi], \quad (2.3)$$

where $L_p^{\ell}(x)$ are the generalized Laguerre polynomials. A word of caution seems to be in order: usually, these modes are presented in terms of two different indices: the azimuthal mode index $\ell = m - n$, which is a topological charge giving the number of 2π -phase cycles around the mode circumference, and $p = \min(m, n)$ is the radial mode index, which is related to the number of radial nodes [26]. However, the form (2.3) will be advantageous in what follows.

The crucial observation is that the LG modes can be represented as superpositions of HG modes, and vice versa. This can be compactly written down as [27]

$$\text{LG}_{mn}(\rho, \varphi) = \sum_{k=0}^{m+n} B_{mn}^k \text{HG}_{m+n-k, k}(x, y) \quad (2.4)$$

where the coefficients are

$$B_{mn}^k = \sqrt{\frac{k!(m+n-k)!}{m!n!2^{n+m}}} \frac{(-i)^k}{k!} \frac{d^k}{dt^k} \left[(1-t)^m (1+t)^n \right] \Big|_{t=0}. \quad (2.5)$$

This looks exactly the same as a Schmidt decomposition for a bipartite quantum system. It is nothing but a particular way of expressing a vector in the tensor product of two inner product spaces [28]. Alternatively, it can be seen as another form of the singular-value decomposition [29], which identifies the maximal correlation directly. In quantum information, the Schmidt coefficients B_{mn}^k convey complete information about the entanglement [30–32]. Here, we intend to assess entanglement in LG beams via the violation of suitably formulated Bell inequalities.

3. CHSH violation for Laguerre–Gauss modes

The CHSH inequality was originally derived for dichotomic variables. However, this inequality, in different forms, has been used in recent times for other kind of variables, as long as one deals with two-valued positive operator-valued measurements [33, 34]. The resulting inequality has already been applied to continuous angular variables [35], as is the case of a particle moving on a ring.

The traditional form of the CHSH inequality applies to dichotomic discrete variables. For continuous variables, the sensible formulation is in terms of the Wigner function, which for a classical beam reads

$$W(\mathbf{x}, \mathbf{p}) = \frac{1}{\lambda^2 \pi^2} \int d^2 \mathbf{x}' e^{2i\mathbf{p} \cdot \mathbf{x}' / \lambda} \langle E^*(\mathbf{x} - \mathbf{x}') E(\mathbf{x} + \mathbf{x}') \rangle, \quad (3.1)$$

with the angular brackets denoting the statistical average. We underline that \mathbf{p} is dimensionless. Although originally introduced to represent quantum mechanical phenomena in phase space [36], the Wigner distribution was established in optics [37] to relate partial coherence with radiometry. Since then, a great number of applications of this function have been reported [38–42]. Note that W has the dimensions of an intensity and it yields a description displaying both the position and the momentum (which in the paraxial approximation has the significance of a scaled angular coordinate) of the intensity of the wave field: in fact, one easily proves that

$$\begin{aligned} \int W(\mathbf{x}, \mathbf{p}) d\mathbf{p} &= I(\mathbf{x}) \equiv \langle E^*(\mathbf{x}) E(\mathbf{x}) \rangle, \\ \frac{1}{\lambda^2 \pi^2} \int W(\mathbf{x}, \mathbf{p}) d\mathbf{x} &= I(\mathbf{p}) \equiv \langle E^*(\mathbf{p}) E(\mathbf{p}) \rangle, \end{aligned} \quad (3.2)$$

with

$$E(\mathbf{p}) = \frac{1}{\lambda^2 \pi^2} \int E(\mathbf{x}) \exp(i\mathbf{p} \cdot \mathbf{x} / \lambda) d\mathbf{x}. \quad (3.3)$$

Thus, the marginals of the Wigner function are the intensity distributions in \mathbf{x} or \mathbf{p} space, respectively.

The CHSH inequality can now be stated in terms of the Wigner function as [33]

$$B = \frac{\pi^2}{4} |W(\alpha, \beta) + W(\alpha, \beta') + W(\alpha', \beta) - W(\alpha', \beta')| < 2, \quad (3.4)$$

where $\alpha = (x, p_x)/\sqrt{2}$ and $\beta = (y, p_y)/\sqrt{2}$. This also follows from the work of Gisin [43], who formulated a Bell inequality for the set of observables with the property $\hat{O}^2 = \mathbb{1}$: as we shall see, the Wigner function appears as the average value of the parity, whose square is unity. Reference [24] presents a detailed study of the violations of (3.4).

For the state LG_{mn} , the normalized Wigner function can be written as

$$W_{mn}^{\text{LG}}(X, P_X; Y, P_Y) = \frac{(-1)^{m+n}}{\pi^2} \exp(-4Q_0) L_m[4(Q_0 + Q_2)] L_n[4(Q_0 - Q_2)], \quad (3.5)$$

where

$$Q_0 = \frac{1}{4}(X^2 + Y^2 + P_X^2 + P_Y^2), \quad Q_2 = \frac{1}{2}(XP_Y - YP_X), \quad (3.6)$$

and we have rescaled the variables as $x \mapsto (w/\sqrt{2})X$ and $p_x \mapsto (\sqrt{2}\lambda/w)P_X$ (and analogously for the y axis). The derivation makes use of the relation (2.4), which is equivalent to a rotation of the Hermite–Gauss modes to a new basis. Once this is realized, then one can use quite elegant properties of the rotation group as discussed in [44].

Let us first look at the simple case of the mode LG_{10} , which reduces to

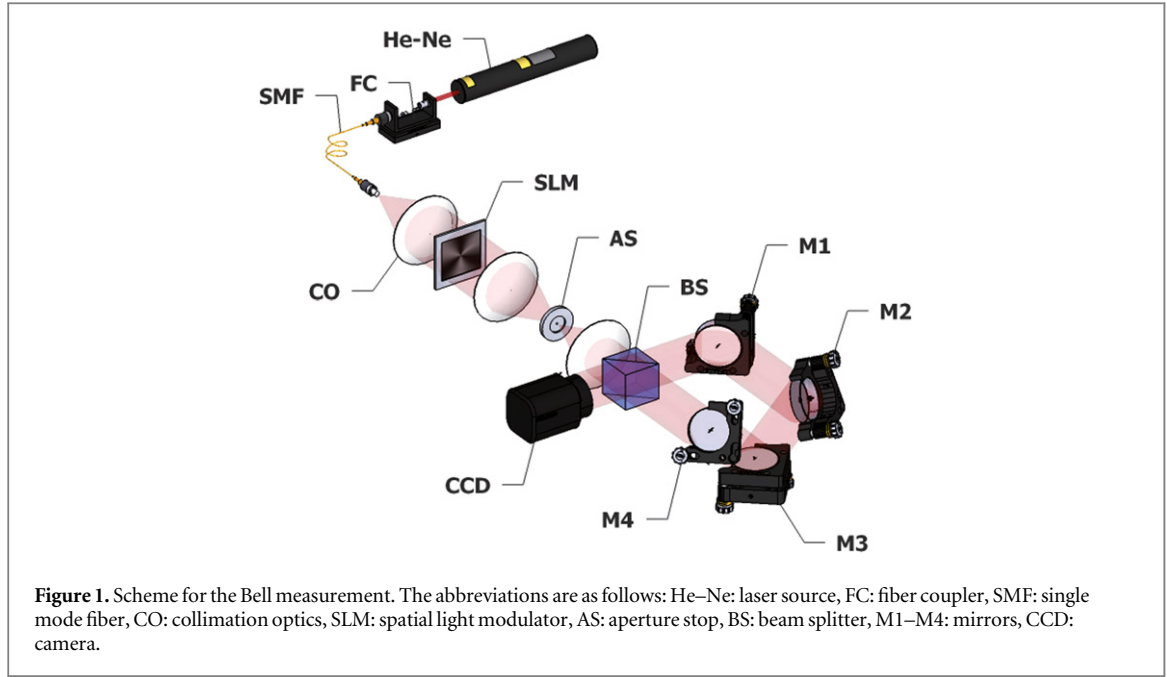
$$W_{10}^{\text{LG}}(X, P_X; Y, P_Y) = \frac{1}{\pi^2} [(P_X - Y)^2 + (P_Y + X)^2 - 1] \exp(-P_X^2 - P_Y^2 - X^2 - Y^2). \quad (3.7)$$

The two measurement settings on one side are chosen to be $\alpha = (X = 0, P_X = 0)$ and $\alpha' = (X' = X, P_X' = 0)$, and the corresponding settings on the other side are $\beta = (Y = 0, P_Y = 0)$ and $\beta' = (Y' = 0, P_Y' = P_Y)$ [45], for which the Bell sum is

$$B = (P_Y^2 - 1)e^{-P_Y^2} + (X^2 - 1)e^{-X^2} - [(P_Y + X)^2 - 1]e^{-(P_Y^2 + X^2)} - 1. \quad (3.8)$$

Upon maximization with respect to X and P_Y , we obtain the maximum Bell violation, $|B_{\text{max}}| \simeq 2.17$, which happens for the choices $X \simeq 0.45$, $P_Y \simeq 0.45$ [24]. For comparison, note that the maximum Bell violation in quantum mechanics through the Wigner function for the two-mode squeezed vacuum state using similar settings is given by $|B_{\text{max}}^{\text{QM}}| \simeq 2.19$ [33].

The Bell violation may be further optimized by a more general choice of settings than those used here. For example, maximizing it with respect to the parameters $\alpha = (X, P_X)$, $\alpha' = (X', P_X')$, $\beta = (Y, P_Y)$, $\beta' = (Y', P_Y')$, one obtains the absolute maximum Bell violation, $|B_{\text{max}}| = 2.24$ which occurs for the choices $X \simeq -0.07$, $P_X \simeq 0.05$, $X' \simeq 0.4$, $P_X' \simeq -0.26$, $Y \simeq -0.05$, $P_Y \simeq -0.07$, $Y' \simeq 0.26$, $P_Y' \simeq 0.4$. The violation also increases with higher orbital angular momentum. This increase with n is analogous to the enhancement of nonlocality in quantum mechanics for many-particle Greenberger–Horne–Zeilinger states [46].



4. Experimental results

We have carried out a direct measurement of the Bell sums for optical beams with different amounts of nonlocal correlations. To understand the measurement, we recall that the Wigner function in quantum optics is often regarded as the average of the displaced parity operator [47]. At the classical level, we can consider the field amplitudes $\mathcal{E}(X, Y)$ as vectors in the Hilbert space of complex-valued functions that are square integrable over a transverse plane. In this space we define linear Hermitian operators

$$\hat{X} : \mathcal{E}(X, Y) \mapsto X\mathcal{E}(X, Y), \quad \hat{P}_X : \mathcal{E}(X, Y) \mapsto -i\frac{\partial}{\partial X}\mathcal{E}(X, Y), \quad (4.1)$$

and analogous ones for the Y variable. Formally, these operators satisfy the canonical commutation relations $[\hat{X}, \hat{P}_X] = [\hat{Y}, \hat{P}_Y] = i$. Therefore, the unitary parity operator is

$$\hat{\Pi}_X \hat{X} \hat{\Pi}_X = -\hat{X}, \quad \hat{\Pi}_X \hat{P}_X \hat{\Pi}_X = -\hat{P}_X, \quad (4.2)$$

which changes $\mathcal{E}(X, Y)$ into $\mathcal{E}(-X, Y)$. The displacement operators are

$$\hat{D}(X, P_X) = \exp[i(P_X \hat{X} + X \hat{P}_X)]. \quad (4.3)$$

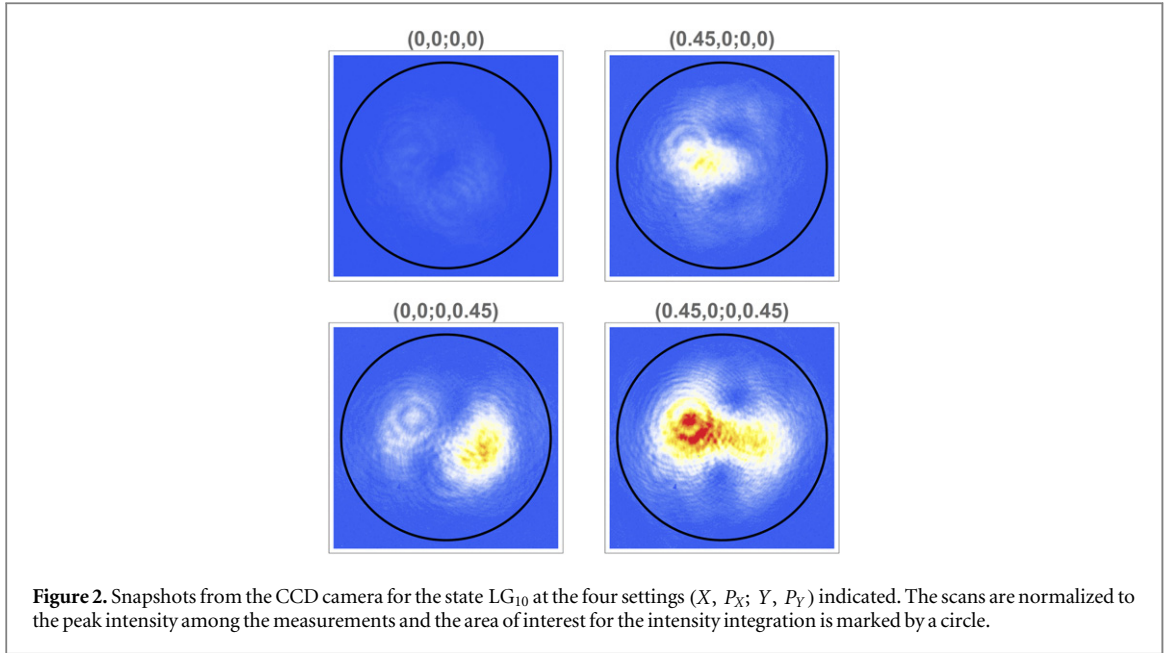
Indeed, with these notations we have

$$W(X, P_X; Y, P_Y) = \frac{4}{\pi^2} \langle \hat{D}(X, P_X) \hat{\Pi}_X \hat{D}^\dagger(X, P_X) \hat{D}(Y, P_Y) \hat{\Pi}_Y \hat{D}^\dagger(Y, P_Y) \rangle. \quad (4.4)$$

Parity measurement can be, in turn, realized by a common-path interferometer with a Dove prism inserted into the optical path [48]. In our setup, sketched in figure 1, the prism was substituted with an equivalent four-mirror Sagnac arrangement [49]. The two copies of the input signal obtained after the input beam splitter are transformed by the mirrors so as to make one copy spatially inverted with respect to the other, prior to combining the beams together. The resulting interference pattern is detected by a CCD camera: figure 2 shows snapshots from the camera for the state LG_{10} at the four settings indicated. The total intensity witnessing parity of the measured beam is computed by spatial integration and this is proportional to the desired Wigner distribution sample after normalization to the overall intensity.

The target signal beams were prepared with digital holograms created by a spatial light modulator (SLM), which modulated a collimated output of a single mode fiber coupled to a He–Ne laser. We also included a 4f-system with an aperture stop to filter the unwanted diffraction orders produced by the SLM. To allow for better flexibility, all the necessary shifts in the X, Y, P_X , and P_Y variables were incorporated into the SLM, so that each Bell measurement was associated with a separate hologram.

The measured beams were coherent superpositions of Hermite–Gaussian beams in the form $a \text{HG}_{10} + ib \text{HG}_{01}$ with $\{a = 1, b = 0\}$, $\{a = 0.4, b = 0.6\}$ and $\{a = 0.5, b = 0.5\}$, respectively. The first and the third are thus a pure Hermite–Gaussian beam and a pure Laguerre–Gaussian vortex beam, respectively. For all the beams we used the settings $X \simeq 0.0$, $P_X \simeq 0.0$, $X' \simeq -0.45$, $P'_X \simeq 0.0$, $Y \simeq 0.0$, $P_Y \simeq 0.0$,



$Y' \simeq 0.0$, $P_Y' \simeq -0.45$ for the evaluation of the Bell sums. The theoretical values of the Bell sums for these are $(-1.91, -2.15, -2.17)$, respectively.

Each measurement was repeated many times with slightly different readings, due to laser intensity instabilities and CCD noise. These effects manifest as measurement errors, which can be estimated from the sample statistics. As the parity measurement requires normalization of the total measured intensity of the interference pattern with respect to the input beam intensity, a separate reading of the input beam intensity was performed. For each optical beam, the mean value of the Bell sum is reported. The results are summarized in figure 3. The Bell correlations grow with the coupling between the basis HG_{10} and HG_{01} modes, with statistically significant violation of the CHSH inequality by the second and third beams, as theoretically predicted.

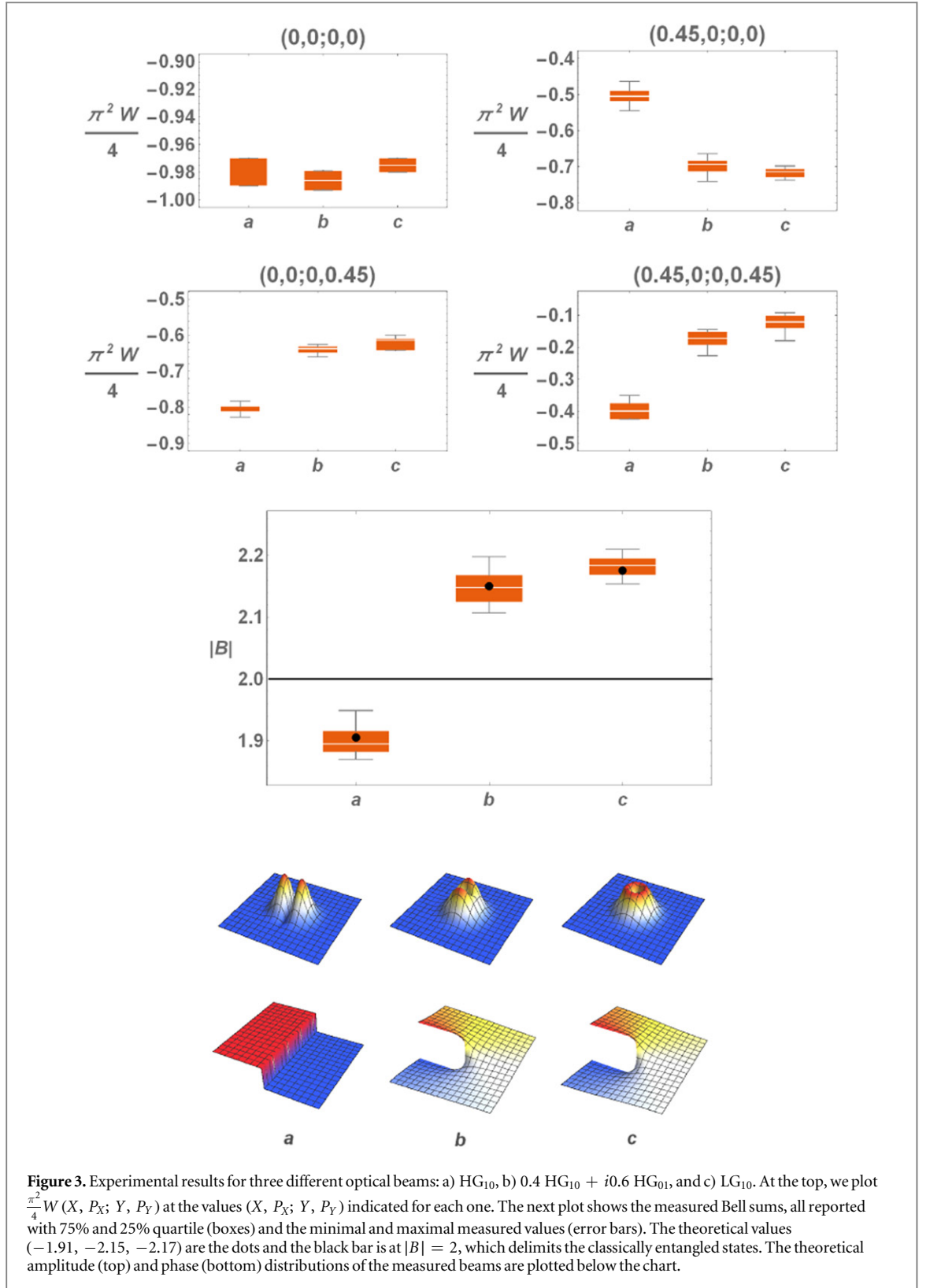
We also show the measured values of the Wigner function. For both HG_{10} and LG_{10} modes, the values of $\pi^2 W(0, 0; 0, 0)$ are quite close to -1 . For classical beams, ours is one of the few measurements on the negativity of the Wigner function, though it has to be anticipated from the corresponding results in quantum optics [50]. We note that very early on, March and Wolf [51] constructed an example of a classical source which exhibited negative a Wigner function.

Finally, we have checked the violation of the CHSH inequality for the beam LG_{20} . A beam with higher topological charge is more sensitive to setup imperfections, hence the Bell sum variation is significantly larger than in the case of LG_{10} . On the other hand, as shown in figure 4, the increasing of the Bell sum for higher orbital angular momentum is clearly demonstrated: the theoretical value for LG_{20} is -2.24 , which agrees pretty well with the experimental results. A study of the Bell violations for LG beams is also presented in [52], although the authors do not employ parity measurements, but Fourier transforms. Note that the Wigner function at the origin of the LG_{20} beam is positive, as expected.

5. Concluding remarks

In short, we have presented an experimental study of nonlocal correlations in classical beams with topological singularities [24]. These correlations between modes are manifested through the violation of a CHSH inequality, which we have detected via direct parity measurements. Such a violation is shown to increase with the value of orbital angular momentum of the beam. As a byproduct of our measurements, we obtain negativity of the Wigner function at certain points in phase space for the HG_{10} and LG_{10} beams. Note that this has implications for similar studies with electron beams, for which vortices have been reported [53, 54].

Though entanglement here does not bear any paradoxical meaning, such as ‘spooky action at a distance’, it still represents a potential resource for classical signal processing. It might be expected that future applications of quantum information processing can be tailored in terms of classical light: the research presented in this work explores one of those options.



Furthermore, our results are relevant not only for a correct understanding of ‘classical entanglement’, but also for bringing out different statistical features of optical beams, since it provides an alternative paradigm to the well developed optical coherence theory. Finally note that nonseparability of classical beams of light holds considerable promise in applications such as metrology and sensing [55–57] and in quantum communications [58]. The tailoring of classical beams which always leads to nonseparable beams has many potential applications [59, 60].

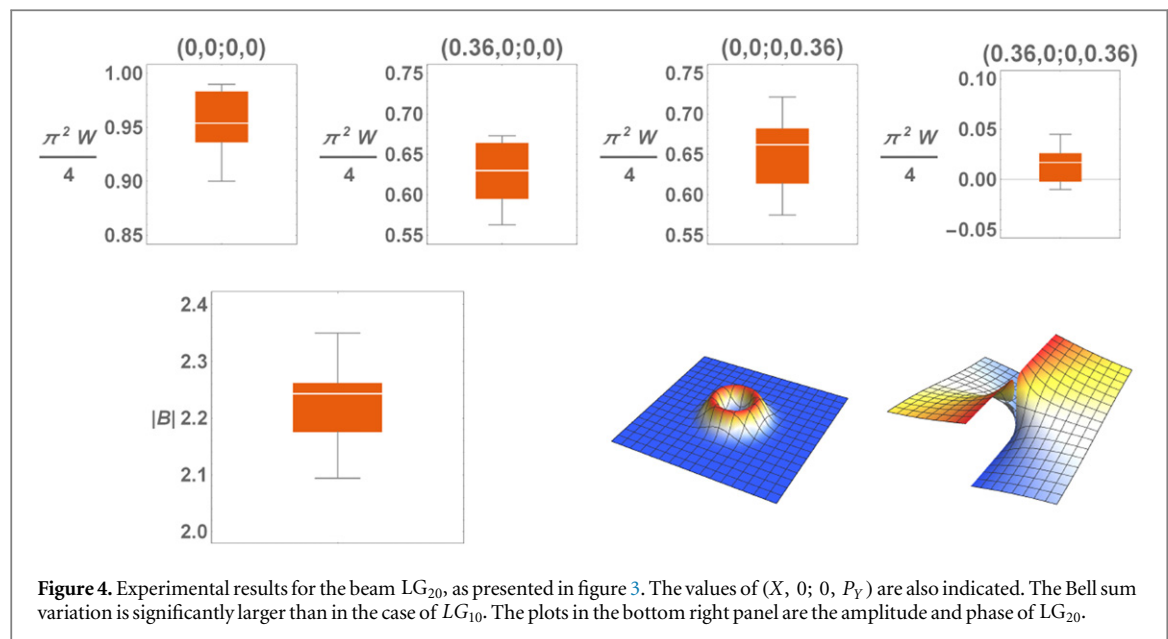


Figure 4. Experimental results for the beam LG_{20} , as presented in figure 3. The values of $(X, 0; 0, P_Y)$ are also indicated. The Bell sum variation is significantly larger than in the case of LG_{10} . The plots in the bottom right panel are the amplitude and phase of LG_{20} .

Acknowledgments

We acknowledge illuminating discussions with Gerd Leuchs, Elisabeth Giacobino, and Andrea Aiello. This work was supported by the Grant Agency of the Czech Republic (Grant 15-031945), the European Social Fund and the State Budget of the Czech Republic POSTUP II (Grant CZ.1.07/2.3.00/30.0041), the IGA of Palacký University (Grant PrF-2015-002), and the UCM-BSCH Program (Grant GR3/14).

References

- [1] Schrödinger E 1935 *Math. Proc. Cambridge Philos. Soc.* **31** 555–63
- [2] Einstein A, Podolsky B and Rosen N 1935 *Phys. Rev.* **47** 777–80
- [3] Horodecki R, Horodecki P, Horodecki M and Horodecki K 2009 *Rev. Mod. Phys.* **81** 865–942
- [4] Bell J 1964 *Physics* **1** 195–200
- [5] Clauser J F, Horne M A, Shimony A and Holt R A 1969 *Phys. Rev. Lett.* **23** 880–4
- [6] Brunner N, Cavalcanti D, Pironio S, Scarani V and Wehner S 2014 *Mod. Phys. Rev.* **86** 419–78
- [7] Werner R F and Wolf M M 2001 *Quant. Inform. Compu.* **1** 1–25
- [8] Töppel F, Aiello A, Marquardt C, Giacobino E and Leuchs G 2014 *New J. Phys.* **16** 073019
- [9] Brunner N, Gisin N and Scarani V 2005 *New J. Phys.* **7** 88
- [10] Aiello A, Töppel F, Marquardt C, Giacobino E and Leuchs G 2015 *New J. Phys.* **17** 043024
- [11] Spreewitz R J C 1998 *Found. Phys.* **28** 361–74
- [12] Ghose P and Mukherjee A 2014 *Rev. Theor. Sci.* **2** 1–4
- [13] Hasegawa Y, Loidl R, Badurek G, Baron M and Rauch H 2003 *Nature* **425** 45–8
- [14] Souza C E R, Huguénin J A O, Milman P and Khoury A Z 2007 *Phys. Rev. Lett.* **99** 160401
- [15] Simon B N, Simon S, Gori F, Santarsiero M, Borghi R, Mukunda N and Simon R 2010 *Phys. Rev. Lett.* **104** 023901
- [16] Borges C V S, Hor-Meyll M, Huguénin J A O and Khoury A Z 2010 *Phys. Rev. A* **82** 033833
- [17] Qian X F and Eberly J H 2011 *Opt. Lett.* **36** 4110–2
- [18] Gabriel C et al 2011 *Phys. Rev. Lett.* **106** 060502
- [19] Qian X F, Little B, Howell J C and Eberly J H 2015 *Optica* **2** 611–5
- [20] Pereira L J, Khoury A Z and Dechoum K 2014 *Phys. Rev. A* **90** 053842
- [21] Fu J, Si Z, Tang S and Deng J 2004 *Phys. Rev. A* **70** 042313
- [22] Lee K F and Thomas J E 2002 *Phys. Rev. Lett.* **88** 097902
- [23] Goyal S K, Roux F S, Forbes A and Konrad T 2013 *Phys. Rev. Lett.* **110** 263602
- [24] Chowdhury P, Majumdar A S and Agarwal G S 2013 *Phys. Rev. A* **88** 013830
- [25] Kagalwala K H, Di Giuseppe G, Abouraddy A F and Saleh B E A 2013 *Nat. Photon.* **7** 72–8
- [26] Karimi E, Boyd R W, de la Hoz P, de Guise H, Řeháček J, Hradil Z, Aiello A, Leuchs G and Sánchez-Soto L L 2014 *Phys. Rev. A* **89** 063813
- [27] Beijersbergen M W, Allen L, van der Veen H and Woerdman J P 1993 *Opt. Commun.* **96** 123–32
- [28] Peres A 1993 *Quantum Theory: Concepts and Methods* (Dordrecht: Kluwer)
- [29] Stewart G W 1993 *SIAM Rev.* **35** 551–66
- [30] Law C K, Walmsley I A and Eberly J H 2000 *Phys. Rev. Lett.* **84** 5304–7
- [31] Agarwal G S and Banerji J 2002 *Opt. Lett.* **27** 800–2
- [32] Sperling J and Vogel W 2011 *Phys. Rev. A* **83** 042315
- [33] Banaszek K and Wódkiewicz K 1999 *Phys. Rev. Lett.* **82** 2009–13
- [34] Ketterer A, Keller A, Coudreau T and Milman P 2015 *Phys. Rev. A* **91** 012106
- [35] Borges C V S, Khoury A Z, Walborn S, Ribeiro P H S, Milman P and Keller A 2012 *Phys. Rev. A* **86** 052107
- [36] Wigner E 1932 *Phys. Rev.* **40** 749–59

- [37] Walther A 1968 *J. Opt. Soc. Am.* **58** 1256–9
- [38] Bastiaans M J 2009 *Phase-Space Optics: Fundamentals and Applications* (New York: McGraw-Hill) 1–44 chap Wigner distribution in Optics
- [39] Galleani L and Cohen L 2002 *Phys. Lett. A* **302** 149–55
- [40] Dragoman D 1997 The Wigner distribution function in optics and optoelectronics *Progress in Optics* ed E Wolf vol 37 (Amsterdam: Elsevier)
- [41] Mecklenbraüker W and Hlawatsch F 1997 *The Wigner Distribution: Theory and Applications in Signal Processing* (Amsterdam: Elsevier)
- [42] Alonso M A 2011 *Adv. Opt. Photon.* **3** 272–365
- [43] Gisin N 1991 *Phys. Lett. A* **154** 201–2
- [44] Simon R and Agarwal G S 2000 *Opt. Lett.* **25** 1313–5
- [45] Zhang L, U'ren A B, Erdmann R, O'Donnell K A, Silberhorn C, Banaszek K and Walmsley I A 2007 *J. Mod. Opt.* **54** 707–19
- [46] Mermin N D 1990 *Phys. Rev. Lett.* **65** 1838–40
- [47] Royer A 1977 *Phys. Rev. A* **15** 449–50
- [48] Mukamel E, Banaszek K, Walmsley I A and Dorrer C 2003 *Opt. Lett.* **28** 1317–9
- [49] Smith B J, Killett B, Raymer M G, Walmsley I A and Banaszek K 2005 *Opt. Lett.* **30** 3365–7
- [50] Schleich W 2000 *Quantum Optics in Phase Space* (Berlin: VCH-Wiley)
- [51] Marchand E W and Wolf E 1974 *J. Opt. Soc. Am.* **64** 1219–26
- [52] Prabhakar S, Reddy S G, Aadhi A, Perumangatt C, Samanta G K and Singh R P 2015 *Phys. Rev. A* **92** 023822
- [53] Verbeeck J, Tian H and Schattschneider P 2010 *Nature* **467** 301–4
- [54] McMorran B J, Agrawal A, Anderson I M, Herzing A A, Lezec H J, McClelland J J and Unguris J 2011 *Science* **331** 192–5
- [55] D'Ambrosio V, Spagnolo N, Del Re L, Slussarenko S, Li Y, Kwek L C, Marrucci L, Walborn S P, Aolita L and Sciarrino F 2013 *Nat. Commun.* **4** 2432
- [56] Töppel F, Aiello A, Marquardt C, Giacobino E and Leuchs G 2014 *New J. Phys.* **16** 073019
- [57] Berg-Johansen S, Töppel F, Stiller B, Banzer P, Ornigotti M, Giacobino E, Leuchs G, Aiello A and Marquardt C 2015 *Optica* **2** 864–8
- [58] D'Ambrosio V, Nagali E, Walborn S P, Aolita L, Slussarenko S and Marrucci L and Sciarrino F 2012 *Nat. Commun.* **3** 961
- [59] Zhan Q and Leger J R 2002 *Opt. Express* **10** 324–31
- [60] Dorn R, Quabis S and Leuchs G 2003 *Phys. Rev. Lett.* **91** 233901